Chapter 13

LHC as an ion collider

Heavy ion collisions were included in the conceptual design of the LHC from an early stage, and collisions between beams of fully stripped lead ions ($^{208}Pb^{82+}$) are scheduled for one year after the start-up of the collider with protons. With the nominal magnetic field of 8.33 T in the dipole magnets, these ions will have a beam energy of 2.76 TeV/nucleon, yielding a total centre-of-mass energy of 1.15 PeV and a nominal luminosity of 1.0×10^{27} cm^{-2} s^{-1}. Collisions between ion beams will be provided principally at Interaction Point 2 for the specialised ALICE detector. However, the CMS and ATLAS detectors also plan to study ion collisions with similar luminosities.

While the major hardware systems of the LHC ring appear compatible with heavy ion operation, the beam dynamics and performance limits with ion beams are quite different from those of protons in a number of respects. The LHC also enters new territory where, for example, the copious nuclear electromagnetic interactions in peripheral collisions of the ions can directly limit luminosity and beam lifetime. While these phenomena are present in RHIC, for example, they are not straightforward to observe and do not limit performance. Yet they become critical in the LHC because of the combination of its unprecedented energy and superconducting magnet technology. It is not possible to make firm predictions about factors that may limit the performance of the LHC with ions. In particular, there are substantial uncertainties concerning some vacuum issues and the ion beam parameters during ramping.

13.1 LHC parameters for lead ions

Some aspects of heavy ion beams are similar to those of proton beams. For example, the nominal emittance of the ions has been chosen so that the ion beams have the same geometric size as the nominal proton beams (at beam energies corresponding to the same magnetic field in the dipole magnets). Thus, the most basic considerations of beam size and aperture will be the same as for protons, implying that this is a safe operational value. Despite this, the physics of ion beams is qualitatively and quantitatively different from that of protons, and the values of some parameters are necessarily very different. There are two reference sets of parameters for the lead ion beams:

2008 JINST 3 S08001

Table 13.1: LHC beam parameters bearing upon the peak luminosity in the nominal ion scheme.

Beam Parameters		**Injection**	**Collision**
Lead ion energy	[GeV]	36'900	574'000
Lead ion energy per nucleon	[GeV]	177.4	2'759
Relativistic "gamma" factor		190.5	2'963.5
Number of ions per bunch		7.0×10^7	7.0×10^7
Number of bunches		592	592
Transverse normalised emittance	[μm]	1.4[a]	1.5
Peak RF voltage (400 MHz system)	[MV]	8	16
Synchrotron frequency	[Hz]	63.7	23.0
RF bucket half-height		1.04×10^{-3}	3.56×10^{-4}
Longitudinal emittance (4σ)	[eV s/charge]	0.7	2.5[b]
RF bucket filling factor		0.472	0.316
RMS bunch length[c]	[cm]	9.97	7.94
Circulating beam current	[mA]	6.12	6.12
Stored energy per beam	[MJ]	0.245	3.81
Twiss function $\beta_x = \beta_y = \beta*$ at IP2	[m]	10.0	0.5
RMS beam size at IP2	[μm]	280.6	15.9
Geometric luminosity reduction factor[d]		-	1
Peak luminosity at IP2	[cm^{-2} s^{-1}]	-	1.0×10^{27}

[a] The emittance at injection energy refers to the emittance delivered to the LHC by the SPS without any increase due to injection errors and optical mismatch.
[b] The baseline operation assumes that the longitudinal emittance is deliberately blown up during, or before, the ramp, in order to reduce the intra-beam scattering growth rates.
[c] Dimensions are given for Gaussian distributions. The real beam will not have a Gaussian distribution, but more realistic distributions do not allow analytic estimates for the IBS growth rates.
[d] The geometric luminosity reduction factor depends on the total crossing angle at the IP.

13.1.1 Nominal ion scheme

A peak luminosity of 1.0×10^{27} cm^{-2} s^{-1} has been the overall performance goal for lead ions for some time [11, 12, 64, 65]. The main parameters of the beams at injection and collision energies are given in table 13.1.

13.1.2 Early ion scheme

The first period of operation of the LHC as a lead-lead collider will be carried out with nominal single bunch parameters but ten times fewer bunches and a larger value of $\beta*$. These relaxed parameters will provide more margin against some of the performance limitations, namely those that depend on the total beam current. The reduced luminosity will nevertheless give access to important physics. The parameters at collision energy for this scheme are given in table 13.2.

2008 JINST 3 S08001

Table 13.2: LHC beam parameters bearing upon the peak luminosity in the early ion scheme. Only those parameters that differ from those in the nominal ion scheme (table 13.1) are shown.

Beam Parameters		**Injection**	**Collision**
Number of bunches		62	62
Circulating beam current	[mA]	0.641	0.641
Stored energy per beam	[MJ]	0.0248	0.386
Twiss function $\beta_x = \beta_y = \beta*$ at IP2	[m]	10.0	1.0
RMS beam size at IP2	[μm]	280.6	22.5
Peak luminosity at IP2	[cm^{-2} s^{-1}]	-	5.40×10^{25}

13.2 Orbits and optical configurations for heavy ions

The optics at IP2, for collisions of ion beams in the ALICE detector, will be quite different from that used for protons, in which $\beta*$ = 10 m, and beams are collided with an angle. For ions, collisions will be head-on, with $\beta*$ with values down to 0.5 m. Moreover, since this value is somewhat smaller than the limit of $\beta*$ = 0.55 m for the high-luminosity p-p collisions at IP2 and IP5, the peak values of β_x and β_y in the insertion quadrupoles will be higher in the ion collision optics. The lower value of $\beta*$ is possible with ions because the separation bumps are smaller (see the following section), leaving more aperture for the increased beam size at the peaks of the beta-functions.

For ion collisions in both IP1 and IP5, the optics can be the same as for protons, or may be adjusted to $\beta*$ = 0.5 m, as in IP2. Elsewhere, the pre-collision optics can be maintained in any IP in which the beams do not collide. Thanks to the modularity and independence of the optics in the various interaction regions, it is in principle straightforward to adapt the optics of the LHC to any set of collision points. However, it should be remembered that switching between the various possible configurations may require some operational time in order to establish the appropriate corrections. In particular, each configuration will contribute differently to the horizontal and vertical dispersion around the ring.

Compared with the nominal proton beams, the relatively low intensities and larger bunch spacing of the lead ion beams lead to weak long-range beam-beam effects which do not, in themselves, require any minimum separation around the interaction points. If these were the only considerations, it might be possible to eliminate the crossing angle entirely. However, this would create additional head-on beam-beam encounters, reducing the beam lifetime. The collisions at additional encounters would also interfere with the trigger for ALICE. Moreover, the ALICE detector has a spectrometer magnet, which is compensated by its own orbit separation bump around IP2. The total separation will be the superposition of this bump and the “external” crossing angle and parallel separation bumps. At the IP, the full crossing angle is given by

$$[\theta_c/\mu\text{rad}] \approx 140 f_{\text{ALICE}} - 340 f_{\text{IP2 bump}},$$

where f_{ALICE} and $f_{\text{IP2 bump}}$ are amplitude factors for the bumps (normalised so that θ_c = -200 μrad for $f_{\text{ALICE}} = f_{\text{IP2 bump}}$=100%). It is desirable to use the minimum separation needed because, with the full separation used for protons, the criteria for minimum aperture are violated. Since the ion collision optics in IR2 has higher maximum values of β_x and β_y in the insertion quadrupoles, the

2008 JINST 3 S08001

need to observe the minimum physical aperture criteria is another strong reason for reducing the separation bump amplitudes in the collision optics.

13.3 Longitudinal dynamics

Nominal longitudinal parameters for lead ions at injection and collision energies are given in table 13.1. The relatively small injected longitudinal emittance of ε_λ = 0.7 eV s/charge is necessary for efficient injection, as long as the 200 MHz capture system (discussed in the Introduction to Chapter 4) is not installed. All parameters given in this chapter assume these conditions. Because of mismatch and nonlinearities, some filamentation to a slightly larger value of emittance after injection is likely. Under these conditions, the bunches occupy about one half of the RF bucket area. However, the relatively short growth times for the longitudinal emittance at nominal intensity imply a further increase in longitudinal emittance if the bunches have to be kept for some time at injection. At some point, ions may start to spill out of the RF bucket. However, since beam-loading will be very small for the foreseen ion beams, a reserve of 50% of the total RF voltage will be available to counter this. Controlled blow up to ε_λ = 2.5 eV s/charge is in any case necessary during the ramp to collision energy, to reduce the growth of the transverse emittances from intra-beam scattering.

13.4 Effects of nuclear interactions on the LHC and its beams

When ultra-relativistic lead ions collide at LHC energies, numerous processes of fragmentation and particle production can occur. Some of these have direct consequences as performance limits for the collider. Besides the hadronic nuclear interactions due to direct nuclear overlap,

$$^{208}Pb^{82+} + {}^{208}Pb^{82+} \xrightarrow{\text{nuclear}} X \tag{13.1}$$

for which the cross section is

$$\sigma_H \approx 8 \text{ barn} \tag{13.2}$$

there is an important class of longer-range, or peripheral, collisions, dominated by electromagnetic interactions. When colliding light ions, the cross sections for these processes are small (some are zero in the case of protons) compared with σ_H. For heavy ions (with $Z \geq 30$), and Pb in particular, the cross sections for these electromagnetic interactions are much larger than σ_H. While simple elastic (Rutherford) scattering and free e^+ e^- pair production are of little consequence, other processes change the charge state or mass of one of the colliding ions, creating a secondary beam emerging from the collision point. For a change, ΔQ, in the charge, Q, and ΔA in the number of nucleons, A, the magnetic rigidity of the secondary beam corresponds to an effective fractional momentum deviation given approximately[1] by

$$\delta(\Delta Q, \Delta A) \approx \frac{1+\Delta A/A}{1+\Delta Q/Q} - 1 \tag{13.3}$$

[1] This assumes that the momentum per nucleon of all final state components — for example, emitted neutrons — in the laboratory frame remains close to its value in the initial state. It is easy to see that the approximation is good for the electron capture process. Detailed calculations show that this holds, in an average sense, to a fairly good approximation in the electromagnetic dissociation processes considered.

2008 JINST 3 S08001

All contributions to the total cross section for ion collisions will, of course, contribute to the total loss rate and resulting beam lifetime. However, certain processes have consequences beyond this, causing concentrated particle losses, heating and finally magnet quenches. An important example is electron capture from pair production, in which a lead nucleus captures an electron (ECPP),

$$^{208}Pb^{82+} + ^{208}Pb^{82+} \xrightarrow{\gamma} ^{208}Pb^{82+} + ^{208}Pb^{81+} + e^{+}. \tag{13.4}$$

Another important effect is electromagnetic dissociation, in which a lead ion first makes a transition to an excited state and then decays with the emission of a neutron, leaving a lighter isotope of lead (EMD),

$$\begin{aligned} ^{208}Pb^{82+} + ^{208}Pb^{82+} &\xrightarrow{\gamma} \; ^{208}Pb^{82+*} \\ &\longrightarrow \; + ^{207}Pb^{82+} + n \end{aligned} \tag{13.5}$$

The total cross section for removal of an ion from the beam is,

$$\sigma_T = \sigma_H + \sigma_{\mathrm{ECPP}} + \sigma_{\mathrm{EMD}} \approx 514\,\mathrm{barn}\,. \tag{13.6}$$

13.5 Intra-beam scattering

Multiple Coulomb scattering within an ion bunch, known as intra-beam scattering (IBS), is a diffusive process that modifies all three beam emittances. IBS is already significant for protons in the LHC, but it is even stronger for lead ion beams of nominal intensity and determines the acceptable longitudinal emittance, particularly at injection from the SPS. As the emittances increase from the initial nominal values, the growth rates due to IBS will decrease. Figure 13.1 shows how the emittance growth times due to IBS depend on longitudinal emittance.

13.6 Synchrotron radiation from lead ions

The LHC is not only the first proton storage ring in which synchrotron radiation plays a noticeable role (mainly as a heat load on the cryogenic system), but also the first heavy ion storage ring in which synchrotron radiation has significant effects on beam dynamics. Surprisingly, perhaps, some of these effects are stronger for lead ions than for protons, because the charges in the nucleus of the ion behave coherently.[2] Quantities such as the energy loss per turn from synchrotron radiation, and the radiation damping time for ions, are obtained from the familiar formulas for electrons by replacing the classical electron radius and the mass by those of the ions. The principal characteristics of the incoherent synchrotron radiation of fully stripped ions of atomic number Z and mass number A can be related to those of protons (assuming the same field in the bending magnets) by,

$$\frac{U_{\mathrm{Ion}}}{U_p} \approx \frac{Z^6}{A^4} \approx 162 \qquad \frac{u^c_{\mathrm{Ion}}}{u^c_p} \approx \frac{Z^3}{A^3} \approx 0.061 \tag{13.7}$$

[2]The nuclear radius being much smaller than relevant wavelengths, the nucleus radiates coherently, like a single charge *Ze*.

2008 JINST 3 S08001

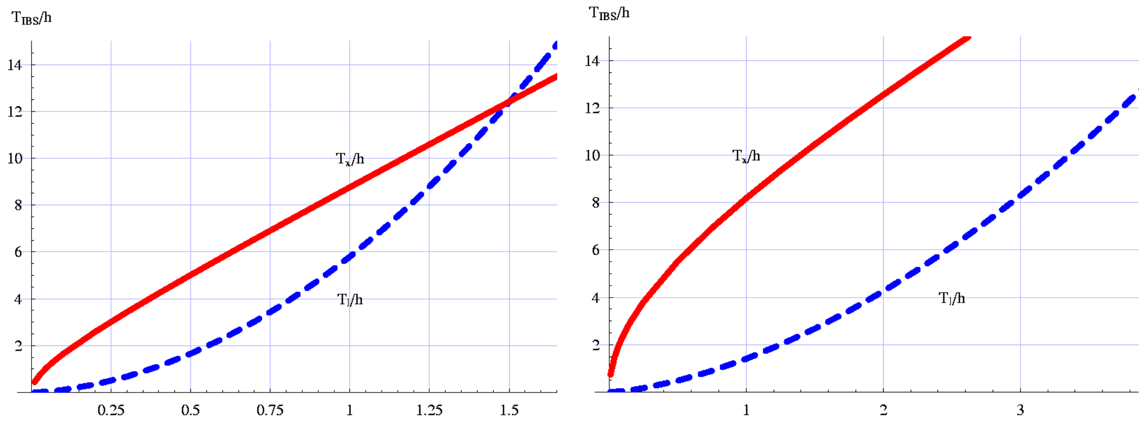

Figure 13.1: Emittance growth times from intra-beam scattering as a function of longitudinal emittance for ^{208} Pb $^{82+}$ at injection (left plot) and collision (right plot) energies. The transverse emittances and beam intensities are taken to have their nominal values, and the total circumferential voltages from the 400 MHz RF system, at injection and collision, are VRF = 8 MV and VRF = 16 MV, respectively. Solid and dashed lines correspond to the growth times for horizontal (μm.rad) and longitudinal emittances (eV.s).

$$\frac{N_{\text{Ion}}}{N_p} \approx \frac{Z^3}{A} \approx 2651 \qquad \frac{\tau_{\text{Ion}}}{\tau_p} \approx \frac{A^4}{Z^5} \approx 0.5, \tag{13.8}$$

where U is the energy lost per ion per turn by synchrotron radiation, u^c is the critical energy of the synchrotron radiation photons, N is the number of photons emitted per turn, and τ is the synchrotron radiation damping time. The numerical values are given for the case of the lead ion $^{208}Pb^{82+}$. It is notable that radiation damping for heavy ions like lead is about twice as fast as for protons, and that the emittance damping times are comparable with the growth times from intra-beam scattering.

2008 JINST 3 S08001